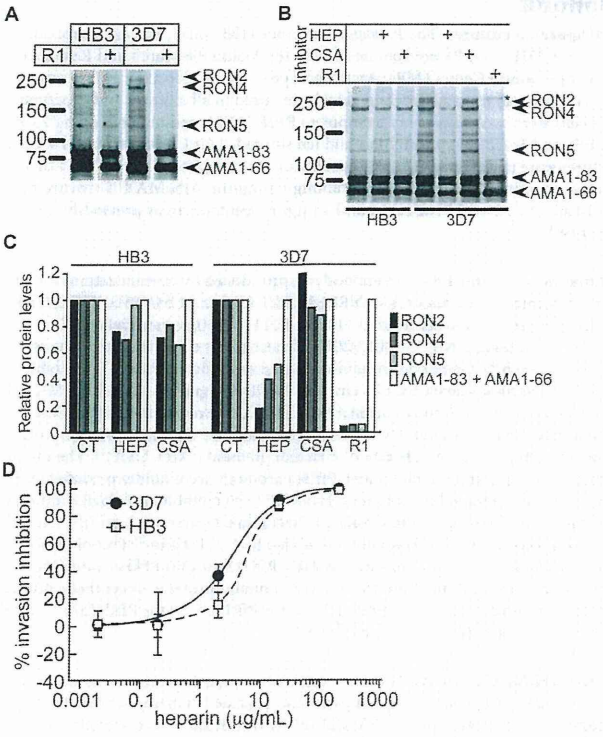

Figure 7 | Clone-specific disruption of the AMA1/RONs complex by heparin contributes little to invasion inhibition. (A), (B) Radiolabeled schizont lysates from the HB3 or 3D7 clones were immunoprecipitated with the 28G2 monoclonal antibody (anti-AMA1) in the presence or absence of 1 mg/mL heparin (HEP), CSA, or the R1 peptide, and then subjected to autoradiographic analysis. The arrowheads indicate the bands that correspond to each molecule. The bands corresponding to RON2 from the HB3 clone exhibited slower mobility on SDS-PAGE than did those from the 3D7 clone. The asterisk in panel B denotes a nonspecific band that did not appear consistently but did not disappear in the presence of the R1 peptide. The molecular masses (kDa) are indicated on the left. (C) Relative protein levels of each RON protein co-immunoprecipitated with AMA-1 in the absence or presence of heparin, CSA, or the R1 peptide. The optical densities of each band were measured with Image J software. Data are shown as the means of two independent experiments. (D) Invasion inhibitory activities of heparin against the *P. falciparum* HB3 and 3D7 clones. Invasion assays were performed in the presence of heparin at a final concentration of 0.02, 0.2, 2, 20, or 200 μg/mL. The percentages of invasion inhibition were calculated by dividing the parasitemia of the test cultures by that of the control cultures, multiplying the result by 100, and then subtracting the result from 100. The results are shown as the means of three independent experiments; the error bars represent standard deviations.

chromatography of mature schizont proteins. Heparin is reportedly capable of binding to various mammalian proteins: coagulation factors, lipoprotein lipases, growth factors, and DNA- and RNA-associated enzymes[29,30]. Although heparin may bind to various types of parasite proteins, as it does in mammals, we found that almost all of the erythrocyte-binding proteins of *P. falciparum* have the capacity to bind to heparin. This finding raises the possibility that the binding of heparin to various erythrocyte-binding proteins leads to their binding inhibition, resulting in invasion inhibition.

Our study also showed direct binding between merozoites and heparin-agarose beads, which strongly suggests that heparin binds directly to the merozoite surface. In addition, immunofluorescence studies demonstrated that the heparin localization was restricted to the apical surface. The intracellular localization of heparin-binding proteins was observed mainly in apical organelles, such as micronemes or rhoptries.

Curiously, although this study and a previous one[10] showed that heparin could bind to MSP1–42, which is localized on the merozoite surface, we did not find co-localization of MSP1 with heparin on the merozoite surface. We speculate that because MSP1–42 forms complexes with other MSP fragments[4], the heparin-binding sites in MSP1–42 may have been masked and inaccessible. In addition, because of its relatively low affinity for MSP1–42, heparin preferentially binds to proteins with higher affinities that are localized on the apical surface of merozoites.

Our data suggest that heparin-binding proteins include the erythrocyte-binding proteins that are localized in the apical organelles and that they are transported to the apical surface. These characteristics are similar to those of the ligand molecules that are associated with junction formation. However, junction formation is mediated by multiple receptor–ligand interactions. To disrupt junction formation, heparin would have to block either the essential interaction or multiple alternative interactions. The former possibility was examined. Formation of the AMA1/RONs complex, one of the few essential types of machinery needed for junction formation, was disrupted by heparin in the 3D7 clone but not in the HB3 clone. However, despite no apparent disruption of the complex, heparin sufficiently blocked the invasion of the HB3 clone, suggesting that complex disruption is not a main target of heparin. In addition, when comparing the two live video microscopic studies of merozoite invasion in the presence of the R1 peptide or heparin, we see that the R1 peptide did not interfere with primary attachment or reorientation but participated in further processes despite the appearance of echinocytosis[31], whereas heparin interfered with reorientation but not with primary attachment[10]. Therefore, these two inhibitors inhibit different invasion processes, with heparin inhibiting molecular events other than AMA1/RONs complex formation.

Our findings support the latter possibility that multiple alternative interactions are involved, because all of the DBL and RBL family members that we tested bound to heparin. A remarkable finding is that heparin bound to PfRH2, PfRH4, and PfRH5, all ligands that mediate sialic acid–independent pathways[7]. This finding suggests that heparin inhibits both sialic acid–dependent and sialic acid–independent pathways. This possibility is consistent with a previous finding that both sialic acid–dependent and –independent invasion of *P. falciparum* merozoites is inhibited to the same degree by heparin[10].

Do all of these interactions really occur on the merozoite surface? To answer this question, we must look at when the different parasite ligands bind to heparin. According to the model proposed by Singh *et al.*[32], the DBL proteins localized in micronemes, but not the RBL proteins localized in rhoptries, are secreted onto the merozoite surface during merozoite egress and subsequently interact with their specific receptors during the invasion. These interactions trigger the secretion of rhoptry proteins to the apical surface. Therefore, the DBL family proteins are accessible to heparin before initial attachment, but the RBL family proteins would be inaccessible. Binding of heparin to the DBL family proteins would then to lead to a blockade of the receptor–ligand interactions, resulting in a failure of the RBL-family proteins to secrete to the surface. Alternatively, the binding of heparin to the DBL family proteins may trigger the secretion of rhoptry proteins before junction formation. However, there is contradictory evidence for PfRH4 and EBA-175 playing equivalent roles in merozoite invasion[33,34]. Further detailed research on the molecular events that surround merozoite invasion is required to fully understand the true targets of heparin.

Our model is consistent with a previous video microscopic observation[10]. According to this previous report, in the presence of heparin, merozoites attach to the erythrocyte surface normally but do not proceed to the next step: deformation of the erythrocyte membrane and/or apical reorientation of the merozoites. We found that

heparin binding was restricted at the apical surface of merozoites, implying that other regions of the merozoite surface normally attach to the erythrocyte surface, a finding that is consistent with the result of the video microscopy. Under normal conditions, this attachment triggers deformation of the erythrocyte membrane at the site of attachment, which is predicted to be the actual mechanism of apical reorientation[35,36]. Yet, in the presence of heparin, membrane deformation is inhibited[10]. Although neither the parasite nor the erythrocyte factors involved in this process have been identified, heparin must interfere with such factors to inhibit membrane deformation. However, some studies have suggested that erythrocyte deformation is not an essential step for merozoite invasion[31,35]. Given that heparin inhibits merozoite invasion almost completely, it must inhibit essential steps. In our model, the binding of heparin to the apically expressed parasite ligands inhibits junction formation between the apical surface of merozoites and the erythrocyte membrane, which is essential for merozoite invasion. Consistent with this model, in the movie data of Boyle *et al.*[10], after attachment to the erythrocyte surface, the merozoites appeared to move and roll on the erythrocyte surface in the presence of heparin, but do not form tight junction. Therefore, our model also fit with these previous observations.

Heparin inhibits the invasion of *Toxoplasma gondii*, which, like *P. falciparum*, belongs to the phylum Apicomplexa. However, a much greater concentration of heparin (IC_{50} > 1.0 mg/mL) is required for invasion inhibition of *T. gondii*, compared with that needed for *P. falciparum* (IC_{50} = 5–10 μg/mL). Moreover, CSA also inhibits the invasion of *T. gondii* at comparable levels to heparin[37]. Given the numerous similarities among host cell invasion mechanisms, the reason for these differences between *T. gondii* and *P. falciparum* is unclear. We assume that the differences are due to the repertoires of ligand molecules used for the parasite invasion. The DBL and RBL families, which were shown to bind to heparin in this study, are specific to *Plasmodium* species. If heparin is primarily targeted to these family members, it should inhibit the host cell invasion of *P. falciparum* merozoites more effectively than that of *T. gondii* tachyzoites.

Several studies have reported that some sulfated polysaccharides inhibit the growth of blood-stage *Plasmodium* parasites *in vitro* and *in vivo*[10–13,15–17,21]. Some compounds to which sulfate groups were artificially added have been reported to have inhibitory effects on parasite growth *in vitro* and *in vivo*[18,19]. These data suggest that the sulfate groups on these polysaccharides and these compounds play an important role in growth inhibition, and may have potential as a new type of antimalarial drugs. Here, we propose a model for the inhibition mechanism by heparin, a representative of the sulfated polysaccharides. However, the question remains: are the structural features or negative charge of sulfated compounds important? In this regard, our data suggest that disaccharide heparin fails to bind to the DBL and RBL proteins, in agreement with previous similar reports[10,11]. Therefore, a polysaccharide structure consisting of at least 5 monosaccharide units with sulfate groups is required for the invasion inhibition.

In summary, here, we show that heparin targets multiple molecules that mediate the parasite invasion of erythrocytes, providing important clues for the development of antimalarial drugs to block the merozoite. Because multiple molecules are not likely to simultaneously acquire resistance to heparin, the risk for emergence of parasites resistant to heparin is assumed to be extremely low. In agreement with this inference, a previous study indicated that no parasite with increased resistance to heparin was selected in the presence of heparin[10]. By identifying the target molecules of heparin, it may be possible to develop compounds that bind those target even more specifically than heparin. Therefore, the result of this study could help in the development of new therapies against malaria.

Methods

P. falciparum cultures. The *P. falciparum* clones HB3, 3D7, and GFP-expressing parasite (3D7HT-GFP) were obtained from the Malaria Research and Reference Reagent Resource Center (MR4; American Type Culture Collection, Manassas, VA). B+ erythrocytes from a single individual were used in all cultures and experiments. The cells were washed twice in incomplete RPMI-1640 medium containing 25 mM HEPES and 367 μM hypoxanthine, and then stored at 50% hematocrit and 4°C. The cultures were maintained at 1%–3% hematocrit in complete medium (CM) that was composed of incomplete medium containing 5 mg/mL AlbuMAX II (Invitrogen, Carlsbad, CA), 27 mM $NaHCO_3$, and 10 μg/mL gentamicin as previously described[38].

Antibodies. The anti-EBA-175 antibody was produced by immunization of rabbits with the synthetic peptides CYKVNEREDERTLTKE and CMNRESDDGELYDEN, which comprise amino acids 1092–1107 and 1117–1130, respectively, of EBA-175 (GenBank Accession No. XP_001349207). These regions overlap the previously reported region[39]. A rabbit was immunized as previously described[21]. The rabbit polyclonal antibody against the C-terminal 19-kDa fragment of MSP1 (MSP1–19) and a rat monoclonal antibody against AMA1 (28G2)[40] were obtained from MR4. The rabbit anti-AMA1-C1 antibody was kindly provided by Drs. Carol A. Long and. Kazutoyo Miura (National Institute of Health, Bethesda, MD, USA)[41]. The rat anti-JESEBL antibody and the rabbit anti-PfRH4 antibody were kindly provided by Dr. Louis H. Miller (National Institute of Health)[42,43]. The rabbit anti-clag3.1 antibody was kindly provided by Dr. Osamu Kaneko (Nagasaki University, Japan)[44]. The rabbit antibody against PfRON2 was kindly provided by Dr. Takafumi Tsuboi (Ehime University, Japan)[26]. The mouse anti-PfRH1, PfRH2a/b, and PfRH5 antibodies were obtained by immunization of mice with recombinant proteins or synthetic peptides, identical to those previously reported: R515 for PfRH1[45], S3 for PfRH2a/b[46], and the peptide LIKCIKNHENDFNKIC for PfRH5[47].

Polysaccharides. Heparin, CSA, and biotinylated heparin were purchased from Sigma-Aldrich (St. Louis, MO) and heparin disaccharide 1-S from Dextra Laboratory (Reading, UK). The R1 peptide VFAEFLPLFSKFGSRMHILK was synthesized (Operon Biotechnologies, Tokyo, Japan).

Invasion inhibition assays. Invasion assays were performed as described previously[48]. Briefly, 3 μL of packed erythrocytes were mixed with 6×10^5 schizonts, which were enriched by the Percoll-sorbitol method 25 h after synchronization with the 5% D-sorbitol method. After being cultured for 20 h, parasitemias of ring-stage parasites were evaluated by using Giemsa-stained culture smears.

Immunofluorescent staining. To detect the binding of merozoites to heparin-agarose beads, purified schizont-stage parasites were suspended in CM. The suspension was then mixed with heparin-agarose beads and 10 mg/mL soluble heparin or CSA and incubated at 37°C, 5% CO_2, and 5% O_2. Parallel cultures were prepared by the addition of fresh erythrocytes to the purified schizonts and monitored for increases in ring forms to determine the optimal time to observe parasite egress. When the number of egressing parasites was estimated to be increasing in the culture, the beads were suspended in 10 mL of ice-cold ICM and centrifuged at 120 × *g* for 10 sec at 4°C to precipitate only the beads. The supernatant containing parasitized erythrocytes and free merozoites was removed. The beads were then washed with ICM three times with centrifugation under the same condition, fixed, and blocked as described previously[49]. After incubation with 5 μM DAPI or 2 μM TO-PRO-3 iodide (Invitrogen) for 1 h at room temperature, the beads were rinsed three times with PBS. Lastly, 3–4 μL of the suspension was spotted onto a glass slide, mounted under a coverslip, and observed under a fluorescent microscope (model BZ-9000; Keyence, Osaka, Jaman) and/or a confocal laser-scanning microscope (LSM510; Carl Zeiss, Oberkochen, Germany).

To detect heparin binding sites on the merozoite surface, a synchronous culture at the late schizont stage was mixed with 30 μg/mL biotinylated heparin and cultured. Parallel cultures were monitored to determine the optimal time to observe parasite egress. When the number of egressing parasites was estimated to be increasing in the cultures, the cultures were centrifuged at 800 × *g* for 5 min at room temperature and washed with ICM once and with PBS twice. The cells were then fixed with phosphate buffer containing 1% paraformaldehyde and 0.1% glutaraldehyde for 20 min on ice and subsequently washed with PBS. After being blocked with 1% bovine serum albumin (BSA) overnight at 4°C, they were incubated with an antibody for 30 min at 37°C. After being washed, the slides were incubated with 2 μg/mL Alexa Fluor 633 goat anti-rabbit IgG (H + L) (Invitrogen) and 5 μg/mL streptavidin–Alexa Fluor 488 (Invitrogen). After being washed, the slides were observed as described above.

To detect the localization of heparin-binding molecules in merozoites, a synchronous culture at the late schizont stage was smeared and fixed with methanol for 5 min at room temperature. After being blocked with 0.3% BSA for 30 min at 37°C, the slides were incubated with 50 μg/mL biotinylated heparin and an antibody for 30 min at 37°C. After being washed, the slides were incubated with secondary antibodies and observed as described above.

Metabolic labeling of parasite proteins. Metabolic labeling of parasite proteins with L-[^{35}S]methionine and L-[^{35}S]cysteine was performed as previously described[50].

Pull-down assays. Pull-down assays were performed as previously described[21] using heparin-agarose, Ni-NTA–agarose, glutathione-Sepharose (GE Healthcare, Buckinghamshire, UK), or protein G-Sepharose beads (GE Healthcare).

Erythrocyte-binding assays. Erythrocyte-binding assays were performed as previously described[50].

Affinity chromatography using a heparin column. To collect mature schizonts containing merozoites, the egress of schizonts was halted by adding E-64 cysteine protease inhibitor (Sigma-Aldrich) to a highly synchronized culture of *P. falciparum* HB3 clone at the schizont stage[51]. After 3–8 h, parasite lysates were prepared by saponin treatment[52] and were solubilized with lysis buffer [10 mM NaH_2PO_4 (pH 6.7) containing 100 mM NaCl, 1 mM EDTA, and 1.0% Triton X-100] and a protease inhibitor cocktail (Roche Diagnostics, Mannheim, Germany) for 1 h at 4°C. After centrifugation at 91,000 × *g* for 1 h at 4°C, the supernatant was diluted with binding buffer [10 mM NaH_2PO_4 (pH 6.7) containing 100 mM NaCl] and applied to a HiTrap heparin HP column (GE Healthcare) that was equilibrated with binding buffer. The column was washed with wash buffer [10 mM NaH_2PO_4 (pH 6.7) containing 100 mM NaCl and 0.1% Triton X-100] and proteins were eluted from the column with a stepwise gradient of 0–1.5 M NaCl or 0–10 mg/mL soluble heparin or CSA in wash buffer. Protein concentrations in each fraction (1.0 mL) were analyzed by using the Protein Quantification Kit-Raid (Dojindo, Kumamoto, Japan).

Immunoblot analysis. Immunoblot analysis was performed as previously described[53].

Immunoprecipitation. Immunoprecipitation was performed as previously described[50]. Briefly, synchronized and purified schizonts were labeled with L-[^{35}S]methionine and L-[^{35}S]cysteine for 3 h. The parasites were harvested by centrifugation and washed once with PBS. Proteins were extracted from the parasite pellet in Lysis buffer containing one of the inhibitors. After centrifugation, the supernatants were preincubated at 4°C for 1 h with an equal volume of protein G-Sepharose beads. Aliquots of the recovered supernatants were diluted with IP buffer [10 mM NaH_2PO_4 (pH 6.7) containing 100 mM NaCl, 0.5% Triton X-100, and 0.5% BSA] containing one of the inhibitors, incubated with an antibody for 2 h, then incubated for 1.5 h at 4°C with 50% protein G-Sepharose beads. After this incubation, the beads were washed twice with NETT buffer [50 mM Tris–HCl (pH 7.4), 0.15 M NaCl, 5 mM EDTA, and 0.5% Triton X-100] containing 0.5% BSA, and three times with NETT. Finally, proteins were eluted from the beads with sodium dodecyl sulfate-polyacrylamide gel electrophoresis (SDS-PAGE) sample buffer and analyzed by autoradiography.

Flow cytometry. Synchronous cultures at the late schizont stage with increasing numbers of ring forms were mixed with 50 μg/mL biotinylated heparin and cultured for 1 h. The cultures were centrifuged at 500 × *g* for 5 min at room temperature to separate free merozoites from erythrocytes. The supernatants containing free merozoites were passed through 1.2-μm filters (Whatman, UK) and centrifuged at 3300 × *g* for 5 min at room temperature. The merozoites were then washed with FACS buffer consisting of PBS containing 2% fetal calf serum and 0.1% sodium azide and were incubated with 10 μg/mL ethidium bromide and 10 μg/mL streptavidin–Alexa Fluor 488 on ice for 1 h. After being washed three times with FACS buffer, the merozoites were analyzed on a FACSCalibur system using Cell Quest software (Becton Dickinson, San Jose, CA). To distinguish merozoites from erythrocytes or cell debris, merozoites were gated by size in the forward scatter channel and by fluorescence in FL2.

1. World Health Organization. *World malaria report: 2012* <www.who.int/malaria> (2012).
2. Aikawa, M., Miller, L. H., Johnson, J. & Rabbege, J. Erythrocyte entry by malarial parasites. A moving junction between erythrocyte and parasite. *J. Cell Biol.* **77**, 72–82 (1978).
3. Dvorak, J. A., Miller, L. H., Whitehouse, W. C. & Shiroishi, T. Invasion of erythrocytes by malaria merozoites. *Science* **187**, 748–750 (1975).
4. Holder, A. A. The carboxy-terminus of merozoite surface protein 1: structure, specific antibodies and immunity to malaria. *Parasitology* **136**, 1445–1456 (2009).
5. Richard, D. *et al.* Interaction between *Plasmodium falciparum* apical membrane antigen 1 and the rhoptry neck protein complex defines a key step in the erythrocyte invasion process of malaria parasites. *J. Biol. Chem.* **285**, 14815–14822 (2010).
6. Srinivasan, P. *et al.* Binding of *Plasmodium* merozoite proteins RON2 and AMA1 triggers commitment to invasion. *Proc. Natl. Acad. Sci. U. S. A.* **108**, 13275–13280 (2011).
7. Tham, W. H., Healer, J. & Cowman, A. F. Erythrocyte and reticulocyte binding-like proteins of *Plasmodium falciparum*. *Trends Parasitol* **28**, 23–30 doi:10.1016/j.pt.2011.10.002 (2012).
8. Dondorp, A. M. *et al.* Artemisinin resistance in *Plasmodium falciparum* malaria. *N. Engl. J. Med.* **361**, 455–467 doi:10.1056/NEJMoa0808859 (2009).
9. Borrmann, S. *et al.* Declining responsiveness of *Plasmodium falciparum* infections to artemisinin-based combination treatments on the Kenyan coast. *PLoS One* **6**, e26005 doi:10.1371/journal.pone.0026005 (2011).
10. Boyle, M. J., Richards, J. S., Gilson, P. R., Chai, W. & Beeson, J. G. Interactions with heparin-like molecules during erythrocyte invasion by *Plasmodium falciparum* merozoites. *Blood* **115**, 4559–4568 (2010).
11. Clark, D. L., Su, S. & Davidson, E. A. Saccharide anions as inhibitors of the malaria parasite. *Glycoconj. J.* **14**, 473–479 (1997).
12. Evans, S. G., Morrison, D., Kaneko, Y. & Havlik, I. The effect of curdlan sulphate on development *in vitro* of *Plasmodium falciparum*. *Trans. R. Soc. Trop. Med. Hyg.* **92**, 87–89 (1998).
13. Butcher, G. A., Parish, C. R. & Cowden, W. B. Inhibition of growth in vitro of *Plasmodium falciparum* by complex polysaccharides. *Trans. R. Soc. Trop. Med. Hyg.* **82**, 558–559 (1988).
14. Xiao, L., Yang, C., Patterson, P. S., Udhayakumar, V. & Lal, A. A. Sulfated polyanions inhibit invasion of erythrocytes by plasmodial merozoites and cytoadherence of endothelial cells to parasitized erythrocytes. *Infect. Immun.* **64**, 1373–1378 (1996).
15. Adams, Y., Smith, S. L., Schwartz-Albiez, R. & Andrews, K. T. Carrageenans inhibit the *in vitro* growth of *Plasmodium falciparum* and cytoadhesion to CD36. *Parasitol. Res.* **97**, 290–294 doi:10.1007/s00436-005-1426-3 (2005).
16. Beuria, M. K. & Das, M. K. Dextran sulfate induced suppression of *Plasmodium berghei* parasitaemia. *Indian J. Exp. Biol.* **29**, 284–285 (1991).
17. Chen, J. H., Lim, J. D., Sohn, E. H., Choi, Y. S. & Han, E. T. Growth-inhibitory effect of a fucoidan from brown seaweed Undaria pinnatifida on *Plasmodium parasites*. *Parasitol. Res.* **104**, 245–250 doi:10.1007/s00436-008-1182-2 (2009).
18. Kisilevsky, R. *et al.* Short-chain aliphatic polysulfonates inhibit the entry of *Plasmodium* into red blood cells. *Antimicrob. Agents Chemother.* **46**, 2619–2626 (2002).
19. Crandall, I. E. *et al.* Sulfated cyclodextrins inhibit the entry of *Plasmodium* into red blood cells. Implications for malarial therapy. *Biochem. Pharmacol.* **73**, 632–642 (2007).
20. Kobayashi, K. *et al.* Application of retrovirus-mediated expression cloning for receptor screening of a parasite. *Anal. Biochem.* **389**, 80–82 (2009).
21. Kobayashi, K. *et al. Plasmodium falciparum* BAEBL binds to heparan sulfate proteoglycans on the human erythrocyte surface. *J. Biol. Chem.* **285**, 1716–1725 (2010).
22. Maier, A. G. *et al. Plasmodium falciparum* erythrocyte invasion through glycophorin C and selection for Gerbich negativity in human populations. *Nat. Med.* **9**, 87–92 (2003).
23. Baum, J. *et al.* Reticulocyte-binding protein homologue 5 - an essential adhesin involved in invasion of human erythrocytes by *Plasmodium falciparum*. *Int. J. Parasitol.* **39**, 371–380 (2009).
24. Kulane, A. *et al.* Effect of different fractions of heparin on *Plasmodium falciparum* merozoite invasion of red blood cells *in vitro*. *Am. J. Trop. Med. Hyg.* **46**, 589–594 (1992).
25. Barragan, A. *et al.* The duffy-binding-like domain 1 of Plasmodium falciparum erythrocyte membrane protein 1 (PfEMP1) is a heparan sulfate ligand that requires 12 mers for binding. *Blood* **95**, 3594–3599 (2000).
26. Cao, J. *et al.* Rhoptry neck protein RON2 forms a complex with microneme protein AMA1 in *Plasmodium falciparum* merozoites. *Parasitol Int* **58**, 29–35 (2009).
27. Collins, C. R., Withers-Martinez, C., Hackett, F. & Blackman, M. J. An inhibitory antibody blocks interactions between components of the malarial invasion machinery. *PLoS Pathog* **5**, e1000273 (2009).
28. Harris, K. S. *et al.* Binding hot spot for invasion inhibitory molecules on *Plasmodium falciparum* apical membrane antigen 1. *Infect. Immun.* **73**, 6981–6989 (2005).
29. Golomb, M., Vora, A. C. & Grandgenett, D. P. Purification of reverse transcriptase from avian retroviruses using affinity chromatography on heparin-sepharose. *J. Virol. Methods* **1**, 157–165 (1980).
30. Rabenstein, D. L. Heparin and heparan sulfate: structure and function. *Nat. Prod. Rep.* **19**, 312–331 (2002).
31. Treeck, M. *et al.* Functional analysis of the leading malaria vaccine candidate AMA-1 reveals an essential role for the cytoplasmic domain in the invasion process. *PLoS Pathog* **5**, e1000322 doi:10.1371/journal.ppat.1000322 (2009).
32. Singh, S., Alam, M. M., Pal-Bhowmick, I., Brzostowski, J. A. & Chitnis, C. E. Distinct external signals trigger sequential release of apical organelles during erythrocyte invasion by malaria parasites. *PLoS Pathog* **6**, e1000746 (2010).
33. Stubbs, J. *et al.* Molecular mechanism for switching of *P. falciparum* invasion pathways into human erythrocytes. *Science* **309**, 1384–1387 (2005).
34. Gaur, D. *et al.* Upregulation of expression of the reticulocyte homology gene 4 in the *Plasmodium falciparum* clone Dd2 is associated with a switch in the erythrocyte invasion pathway. *Mol. Biochem. Parasitol.* **145**, 205–215 (2006).
35. Gilson, P. R. & Crabb, B. S. Morphology and kinetics of the three distinct phases of red blood cell invasion by *Plasmodium falciparum* merozoites. *Int. J. Parasitol.* **39**, 91–96 doi:10.1016/j.ijpara.2008.09.007 (2009).
36. Lew, V. L. & Tiffert, T. Is invasion efficiency in malaria controlled by pre-invasion events? *Trends Parasitol* **23**, 481–484 doi:10.1016/j.pt.2007.08.001 (2007).
37. Carruthers, V. B., Hakansson, S., Giddings, O. K. & Sibley, L. D. *Toxoplasma gondii* uses sulfated proteoglycans for substrate and host cell attachment. *Infect. Immun.* **68**, 4005–4011 (2000).
38. Radfar, A. *et al.* Synchronous culture of *Plasmodium falciparum* at high parasitemia levels. *Nat Protoc* **4**, 1828–1844 (2009).

39. Sim, B. K. *et al.* Primary structure of the 175 K *Plasmodium falciparum* erythrocyte binding antigen and identification of a peptide which elicits antibodies that inhibit malaria merozoite invasion. *J. Cell Biol.* **111**, 1877–1884 (1990).
40. Narum, D. L. & Thomas, A. W. Differential localization of full-length and processed forms of PF83/AMA-1 an apical membrane antigen of *Plasmodium falciparum* merozoites. *Mol. Biochem. Parasitol.* **67**, 59–68 (1994).
41. Kennedy, M. C. *et al. In vitro* studies with recombinant *Plasmodium falciparum* apical membrane antigen 1 (AMA1): production and activity of an AMA1 vaccine and generation of a multiallelic response. *Infect. Immun.* **70**, 6948–6960 (2002).
42. Mayer, D. C. *et al.* Polymorphism in the *Plasmodium falciparum* erythrocyte-binding ligand JESEBL/EBA-181 alters its receptor specificity. *Proc. Natl. Acad. Sci. U. S. A.* **101**, 2518–2523 (2004).
43. Gaur, D. *et al.* Recombinant *Plasmodium falciparum* reticulocyte homology protein 4 binds to erythrocytes and blocks invasion. *Proc. Natl. Acad. Sci. U. S. A.* **104**, 17789–17794 (2007).
44. Kaneko, O. *et al.* Apical expression of three RhopH1/Clag proteins as components of the *Plasmodium falciparum* RhopH complex. *Mol. Biochem. Parasitol.* **143**, 20–28 (2005).
45. Triglia, T., Tham, W. H., Hodder, A. & Cowman, A. F. Reticulocyte binding protein homologues are key adhesins during erythrocyte invasion by *Plasmodium falciparum*. *Cell Microbiol* **11**, 1671–1687 (2009).
46. Rayner, J. C., Galinski, M. R., Ingravallo, P. & Barnwell, J. W. Two *Plasmodium falciparum* genes express merozoite proteins that are related to *Plasmodium vivax* and *Plasmodium yoelii* adhesive proteins involved in host cell selection and invasion. *Proc. Natl. Acad. Sci. U. S. A.* **97**, 9648–9653 (2000).
47. Hayton, K. *et al.* Erythrocyte binding protein PfRH5 polymorphisms determine species-specific pathways of *Plasmodium falciparum* invasion. *Cell Host Microbe* **4**, 40–51 (2008).
48. Kaneko, O., Soubes, S. C. & Miller, L. H. *Plasmodium falciparum*: invasion of *Aotus* monkey red blood cells and adaptation to *Aotus* monkeys. *Exp. Parasitol.* **93**, 116–119 (1999).
49. Kato, K., Sudo, A., Kobayashi, K., Tohya, Y. & Akashi, H. Characterization of *Plasmodium falciparum* protein kinase 2. *Mol. Biochem. Parasitol.* **162**, 87–95 (2008).
50. Kaneko, O., Fidock, D. A., Schwartz, O. M. & Miller, L. H. Disruption of the C-terminal region of EBA-175 in the Dd2/Nm clone of *Plasmodium falciparum* does not affect erythrocyte invasion. *Mol. Biochem. Parasitol.* **110**, 135–146 (2000).
51. Boyle, M. J. *et al.* Isolation of viable *Plasmodium falciparum* merozoites to define erythrocyte invasion events and advance vaccine and drug development. *Proc. Natl. Acad. Sci. U. S. A.* **107**, 14378–14383 (2010).
52. Benting, J., Mattei, D. & Lingelbach, K. Brefeldin A inhibits transport of the glycophorin-binding protein from *Plasmodium falciparum* into the host erythrocyte. *Biochem. J.* **300 (Pt 3)**, 821–826 (1994).
53. Hirano, H. & Watanabe, T. Microsequencing of proteins electrotransferred onto immobilizing matrices from polyacrylamide gel electrophoresis: application to an insoluble protein. *Electrophoresis* **11**, 573–580 (1990).

Acknowledgments

This study was supported by a JSPS Research Fellowship for Young Scientists, Grants-in-Aid for Young Scientists, and Scientific Research on Innovative Areas (3308) from the Ministry of Education, Culture, Science, Sports, and Technology (MEXT) and for Research on global health issues from the Ministry of Health, Labour and Welfare of Japan, Bio-oriented Technology Research Advancement Institution (BRAIN), The Naito Foundation, The Mochida Memorial Foundation for Medical and Pharmaceutical Research, and the Program to Disseminate Tenure Tracking System from the Japan Science and Technology Agency (JST). We thank Dr. Louis H. Miller for providing the antibodies against JESEBL and PfRH4; Dr. Osamu Kaneko for providing the antibody against clag3.1 and for instruction in metabolic labeling methods of parasite proteins; Drs. Carol A. Long and Kazutoyo Miura for providing the rabbit anti-AMA1-C1 antibody; and Dr. Takafumi Tsuboi for providing the rabbit antibody against PfRON2. We also thank MR4 for providing us with malaria parasites, contributed by Drs. Thomas E. Wellems, Arthur Talman, and Robert Sinden, and antibodies, contributed by Drs. David C. Kaslow and Alan Thomas.

Author contributions

K.Kobayashi and K.Kato designed the experiments. K.Kobayashi and R.T. carried out the experiments and analyzed the data. H.T., T.S., A.I., H.G., F.C.R., T.I., T.H. and H.A. contributed to the data analysis and discussion. K.Kobayashi and K.Kato wrote the manuscript. K. Kato supervised the study.

Additional information

Competing financial interests: The authors declare no competing financial interests.

How to cite this article: Kobayashi, K. *et al.* Analyses of Interactions Between Heparin and the Apical Surface Proteins of *Plasmodium falciparum*. *Sci. Rep.* 3, 3178; DOI:10.1038/srep03178 (2013).

Parasitol Res (2013) 112:4169–4176
DOI 10.1007/s00436-013-3608-8

ORIGINAL PAPER

Effects of dextran sulfates on the acute infection and growth stages of *Toxoplasma gondii*

Akiko Ishiwa · Kyousuke Kobayashi · Hitoshi Takemae · Tatsuki Sugi · Haiyan Gong · Frances C. Recuenco · Fumi Murakoshi · Atsuko Inomata · Taisuke Horimoto · Kentaro Kato

Received: 19 June 2013 / Accepted: 2 September 2013 / Published online: 6 October 2013

Abstract *Toxoplasma gondii* is one of the most prevalent parasites, causing toxoplasmosis in various warm-blooded animals, including humans. Because of the broad range of hosts susceptible to *T. gondii*, it had been postulated that a universal component of the host cell surface, such as glycosaminoglycans (GAGs), may act as a receptor for *T. gondii* infection. Carruthers et al. (Infect Immun 68:4005–4011, 2000) showed that soluble GAGs have also been shown to disrupt parasite binding to human fibroblasts. Therefore, we investigated the inhibitory effect of GAGs and their analogue dextran sulfate (DS) on *T. gondii* infection. For up to 24 h of incubation after inoculation of *T. gondii*, the inhibitory effect of GAGs on *T. gondii* infection and growth inside the host cell was weak. In contrast, DS markedly inhibited *T. gondii* infection. Moreover, low molecular weight DS particularly slowed the growth of *T. gondii* inside host cells. DS10 (dextran sulfate MW 10 kDa) was the most effective agent in these in vitro experiments and was therefore tested for its inhibitory effects in animal experiments; infection inhibition by DS10 was confirmed under these in vivo conditions. In this report, we showed that DSs, especially DS10, have the potential of a new type of drug for toxoplasmosis.

A. Ishiwa · H. Takemae · T. Sugi · F. C. Recuenco · K. Kato (✉)
National Research Center for Protozoan Diseases, Obihiro University of Agriculture and Veterinary Medicine, Inada-cho, Obihiro, Hokkaido 080-8555, Japan
e-mail: kkato@obihiro.ac.jp

A. Ishiwa · H. Takemae · T. Sugi · H. Gong · F. C. Recuenco · F. Murakoshi · A. Inomata · T. Horimoto · K. Kato
Department of Veterinary Microbiology, Graduate School of Agricultural and Life Sciences, The University of Tokyo, 1-1-1 Yayoi, Bunkyo-ku, Tokyo 113-8657, Japan

K. Kobayashi
Department of Host–Parasite Interaction, Division of Microbiology and Immunology, Institute of Medical Science, University of Tokyo, 4-6-1 Shirokanedai, Minato-ku, Tokyo 108-8639, Japan

Introduction

Toxoplasma gondii is one of the most abundant protozoan parasites and belongs to the phylum Apicomplexa. The prevalence of *T. gondii* in humans and domestic animals is very high worldwide (Tenter et al. 2000). *T. gondii* can invade almost all mammalian and avian cells, suggesting that various warm-blooded animals and birds may be intermediate hosts, although only animals that belong to Felidae can be definitive hosts. After infection, *T. gondii* causes toxoplasmosis at the rapid growth step; *T. gondii* subsequently forms cysts in the brain and other tissues of the intermediate host. In humans, infection occurs by eating raw or insufficiently cooked meat that is contaminated with *T. gondii* cysts or foods contaminated with soil containing *T. gondii* oocysts shed from infected cats. Infection can also occur via the placenta in pregnant women. Acute toxoplasmosis can be fatal in immunocompromised individuals and can cause severe birth defects or abortion during the first trimester of pregnancy (Black and Boothroyd 2000). Several drugs such as antifolate and clindamycin are effective for the treatment of toxoplasmosis (Katlama et al. 1996); however, in an effort to reduce the risks of side effects and the emergence of drug-resistant strains, novel drugs whose mechanism of action differs from that of preexisting drugs are actively sought. In this study, we assessed the possibility of using sulfated polysaccharides as a new type of drug to treat toxoplasmosis.

Because *T. gondii* tachyzoites can invade a wide range of intermediate host cells, it is thought that *Toxoplasma* might recognize many components of the extracellular matrix or widely distributed surface molecules, such as proteoglycans. Glycosaminoglycan (GAG) moieties on heparan sulfate proteoglycans

(HSPGs) decorate the surfaces of the membranes of nearly all vertebrate cell lineages, and a variety of pathogens have evolved strategies for their recognition by GAG, including *Chlamydia* (Zhang and Stephens 1992), *Trypanosoma cruzi* (Ortega-Barria and Pereira 1991), and *Plasmodium* (Pancake et al. 1992). GAG recognition is also involved in cell attachment by *Toxoplasma* based on the observations that low concentrations of GAGs increase the invasion of human fibroblasts and that mutant CHO cells that lack cell surface-sulfated proteoglycans are less susceptible to invasion (Carruthers et al. 2000). In several studies, *T. gondii* tachyzoites were reported to interact with several types of GAGs on a wide range of human cell types (Ortega-Barria and Boothroyd 1999; Carruthers et al. 2000). In Ortega-Barria's report, the researchers analyzed different kinds of sulfated oligosaccharides, including compounds derived from seaweed and synthetic compounds, and demonstrated that soluble GAGs can disrupt parasite binding to human fibroblasts. Accordingly, in this report, we investigated whether different kinds of sulfated polysaccharides could disrupt the rapid growth cycle of *T. gondii* tachyzoites in host cells and in an animal host, with a view of determining whether these compounds could serve as a future drug type for the treatment of toxoplasmosis.

Materials and methods

Polysaccharides

The following polysaccharides, purchased from Sigma-Aldrich (St. Louis, MO), were used in this study: heparin, chondroitin sulfate A (CSA), and C (CSC); various molecular weight dextran sulfates (DSs) (MW 500, 20, 10, and 5 kDa); and dextran (DX) (MW 300 kDa).

Parasite strains

Wild-type *T. gondii* RH (Sugi et al. 2009) strain and *T. gondii* RH strain 2F (Dobrowolski and Sibley 1996) were used in this study. The parasites were maintained in monolayers of Vero cells, as described elsewhere (Sugi et al. 2009).

Cytotoxicity analysis

The MTT method was performed to assess cytotoxicity of various polysaccharides used in this study as described previously (Jones-Brando et al. 2006) with minor changes. Briefly, Vero cells were seeded in 96-well plates. After an overnight culture step, cells were treated with increasing concentrations of the polysaccharide samples used in this study. After 21 h of treatment step, the MTT stock solution was added to each well (final 0.5 mg/ml). After 3 h of incubation at 37 °C, the medium was removed and 100 μl of DMSO was added to each well to solubilize the formazon and the absorbance was measured at 595 nm.

In vitro invasion and growth inhibition assay

To use in vitro assays, Vero cells were seeded into 96-well plates and incubated for 16 h. Freshly lysed host cells infected with *T. gondii* tachyzoites were prepared, and the lysate was filtered through a 5-μm filter to remove host cell debris and obtain a *T. gondii* tachyzoite suspension. This suspension was washed with fresh assay medium (DMEM plus 1 % FCS, 20 mM HEPES, and 0.2 % NaH_2CO_3), and the parasite density was measured with a hemocytometer and adjusted for in vitro analysis. The number of *T. gondii* tachyzoites was quantified by colorimetric detection of β-galactosidase (β-Gal) activity expressed by the parasite strain 2F as previously described (Eustice et al. 1991). In vitro "invasion and/or growth inhibition" assays were performed as follows: for the "invasion and growth inhibition" assay, purified parasites were incubated with Vero cell monolayers in assay medium containing various concentrations of polysaccharide samples for 24 h at 37 °C. On the other hand, for the "invasion or growth inhibition" assay, tachyzoites were incubated with host cell monolayers in the assay medium containing polysaccharides for 30 min at 37 °C ("invasion inhibition"), and after extensively washing with PBS to remove uninfected tachyzoites, fresh assay medium without polysaccharide was applied and the tachyzoites were incubated for up to 24 h. For the "growth inhibition" analysis, parasites were incubated in the assay medium without polysaccharides for 30 min at 37 °C, then extensively washed with PBS, and incubated with polysaccharide-containing assay medium for up to 24 h. For all of the in vitro inhibition analyses, the monolayers were extensively washed with PBS and lysed, and then β-gal activity was determined by using the substrate chlorophenol red β-D-galactopyranoside (Eustice et al. 1991). In this study, an enhanced β-galactosidase assay kit (CPRG type) (Genlantis Inc., San Diego, CA) was used for the β-galactosidase assay according to the manufacturer's protocol.

Validation of the possibility of direct inhibition of β-galactosidase activity

To validate the possibility that polysaccharides used in this study may directly inhibit β-galactosidase activity, polysaccharide stock solutions (50 mg/ml in lysis buffer of β-galactosidase assay) were serially diluted with lysis buffer and mixed with a constant amount of parasite lysate, following the colorimetric experiment as described in the "In vitro invasion and growth inhibition assay" section.

Animal experiments

Five-week-old female BALB/c mice (SLC, Shizuoka, Japan) were used in this study. For the in vivo infection analysis, tachyzoites of wild-type *T. gondii* RH were collected from the freshly lysed infected host cell monolayer, filtered through a 5-μm pore filter, and counted with a hemocytometer. Then, 1.0×10^3 tachyzoites were inoculated into mice intraperitoneally. Three mice per groups were used in this experiment. Dextran sulfate (MW 10 kDa; termed DS10 from this point) was administered. DS10 (2.5 mg) was administrated to each mouse via the intraperitoneal route at the same time as the parasite inoculation. For the control groups, PBS was injected intraperitoneally instead of DS10. The mice were monitored daily and their vital conditions were recorded. In animal experiments, to quantify the parasite numbers in the tissues of infected mice, three mice per group were used per experiment and experiments were performed in triplicate. Prior to these experiments, a preliminary experiment was performed to determine the upper concentration limit of DS10 that could be administered without causing harmful effects to mice. Animal experiments described in this report were officially approved by the Ethical Committee of The University of Tokyo, and all animal experiments were performed in The University of Tokyo.

Quantification of *T. gondii* tachyzoites in *T. gondii*-infected mouse organs

In this test, 10^3 tachyzoites were inoculated intraperitoneally with and without 2.5 mg of DS10. Three days after inoculation, the mice were euthanized and the lungs and liver were collected for parasite quantification. The parasite load per 1 mg of tissue was quantified by using a quantitative real-time PCR system, as described elsewhere (Huynh and Carruthers 2006). Tissues collected from the infected mice were weighed and used for genomic DNA isolation with QIA amp (QIAGEM, Hilden, Germany), according to the manufacturer's protocol. To detect *T. gondii*-specific DNA, the primer pair TOX-9 and TOX-11 was used (Reischl et al. 2003).

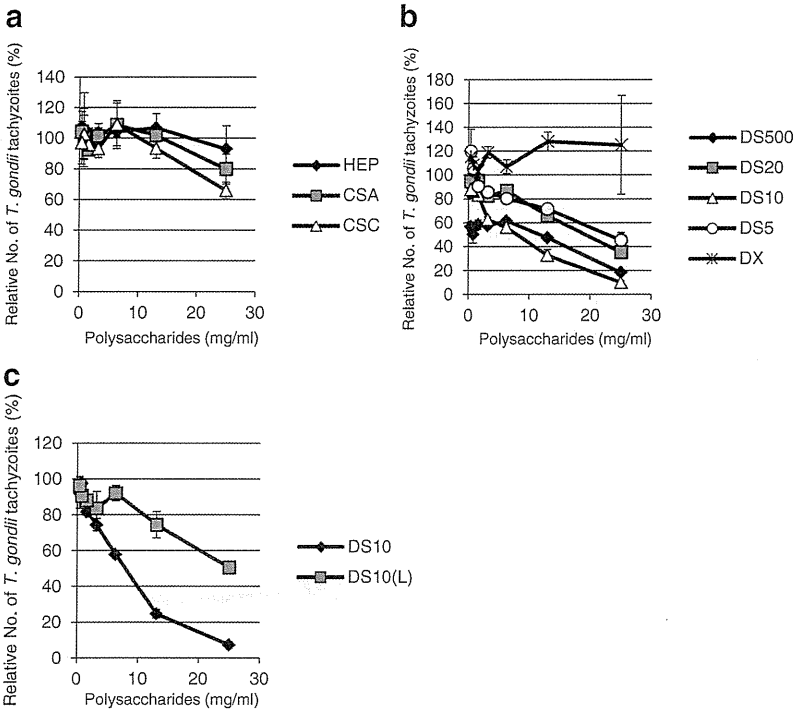

Fig. 1 Invasion and growth inhibition analysis by using a β-galactosidase assay. Purified *T. gondii* tachyzoites were incubated with host cells with or without various (sulfated) polysaccharides. **a** Various glycosaminoglycans were added and incubated for 24 h with *T. gondii* tachyzoites. Heparin (HEP, represented by *diamonds*), chondroitin sulfate A (CSA, represented by *rectangles*), and chondroitin sulfate C (CSC, represented by *triangles*) were then added. **b** Various molecular weights of dextran sulfates (DS) or dextran (DX), nonsulfated polysaccharide, were added and incubated for 24 h with *T. gondii* tachyzoites. Dextran sulfate MW 500 kDa (DS500, represented by *diamonds*), DS MW 20 kDa (DS20, represented by rectangles), DS MW 10 kDa (DS10, represented by *triangles*), DS MW 5 kDa (DS5, represented by *circles*), and dextran MW 300 kDa (DX, represented by *asterisks*) were then added. **c** Two types of dextran sulfate MW10 (highly sulfated or low sulfated) were incubated for 24 h with *T. gondii* tachyzoites. After the 24-h incubation, the 96-well plate was washed three times with PBS and *T. gondii* growth was assessed by using the β-galactosidase assay. *Diamonds* represent high-sulfated DS10; *rectangles* represent low-sulfated dextran sulfate (DS10L)

Results

Effects of various sulfated polysaccharides on *T. gondii* tachyzoite infection and/or growth inside host cells

A previous study reported that high concentrations of sulfated polysaccharides, such as GAGs and dextran sulfate, can inhibit the attachment step of the *T. gondii* infection cycle (Carruthers et al. 2000). Here, we further investigated the effects of various sulfated polysaccharides on the infection and rapid growth stages of *T. gondii* tachyzoites by incubating the polysaccharides with *T. gondii* tachyzoites for a longer time, such that they could influence not only attachment and invasion, but also growth inside the host cell by endodyogeny. First, we analyzed the effect of GAGs, which are expressed on various cell surfaces and are thought to function as receptors for *T. gondii* infection. Heparin, CSA, and CSC all inhibited *T. gondii* tachyzoites' growth in a dose-dependent manner (Fig. 1a). Next, we analyzed the effect of dextran sulfate. In this study, various molecular weight DS samples were used (Fig. 1b), namely high molecular weight DS (DS500; MW 500 kDa) and three low molecular weight DS samples (DS20, MW 20 kDa; DS10, MW 10 kDa; and DS5, MW 5 kDa), and their activities were compared. As shown in Fig. 1b, DS administration caused a remarkable deceleration of the growth of *T. gondii* tachyzoites, whereas the nonsulfated dextran sample showed no inhibitory effect on the infection or growth of *T. gondii* tachyzoites. The most effective DS sample analyzed in this study was DS10. We had thought that the higher molecular weight polysaccharides would have a greater effect than the lower molecular weight polymers; however, this result suggests that there may be an optimum molecular size for these polysaccharides to exhibit optimal invasion and/or growth inhibition activity.

We also hypothesized that high-sulfated polysaccharides would show a greater effect than low-sulfated polysaccharides. To test this hypothesis, we compared the activities of a high-sulfated dextran sulfate (DS10) and a low-sulfated dextran sulfate (DS10-L). The average molecular weights of both of these samples were 10 kDa, and the sulfation rates were approximately 17 % (DS10) and 8–13 % (DS10-L) (manufacturer's information). The high-sulfated DS10 showed a markedly greater effect than its low-sulfated counterpart (Fig. 1c), confirming that the contents of the sulfated group were critical for this activity, at least in the case of dextran sulfate. Moreover, because various polysaccharides were administrated at high concentrations in these experiments, we also confirmed that these polysaccharides do not cause harmful effects under these experimental conditions by the MTT assay (Fig. 2a, b).

Does dextran sulfate affect the acute growth cycle, attachment and invasion, or the growth stage *T. gondii* tachyzoites in host cells?

As shown in Fig. 1, various sulfated polysaccharides, GAGs and DSs, inhibited the growth rate of *T. gondii* tachyzoites when incubated with these tachyzoites for up to 24 h. The length of this incubation time (24 h) was sufficient to study not only the invasion but also the growth by endodyogeny of the *T. gondii* tachyzoites inside the host cells. A previous study indicated that GAGs and DS can effectively inhibit parasite attachment to the host cell, but our results suggest that the effects of GAGs on parasite attachment are small when incubated for up to 24 h. Moreover, the results shown in Fig. 1a suggest that the influence of GAGs on parasite growth inside host cells may also be small. In contrast, DS samples showed potent inhibitory effects on *T. gondii* invasion and reduced the *T. gondii* growth rate during the 24-h incubation (Fig. 1b). We, therefore, sought to confirm the influence of various molecular weight DSs on the invasion and growth (endodyogeny) steps, respectively. The high molecular weight DS (500 kDa) and low molecular weight DSs (5, 10, and 20 kDa) produced different

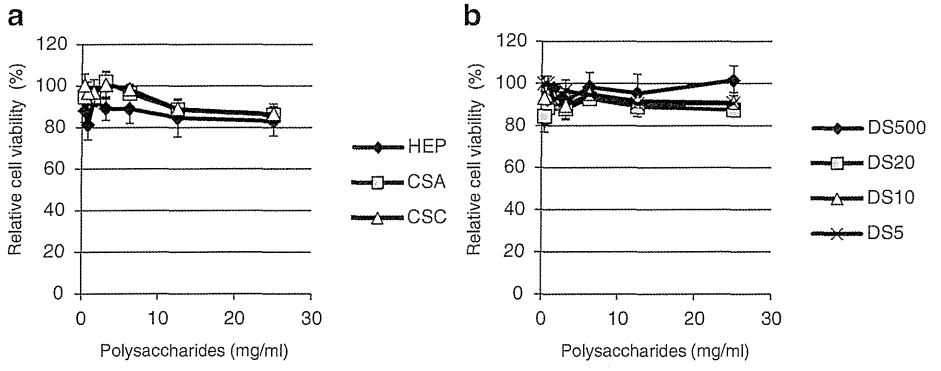

Fig. 2 Cytotoxicity assays. Vero cells were incubated for 24 h in the assay medium containing increasing concentrations of various polysaccharides. After 24 h of incubation, cell viability was quantified by the MTT assay. **a** Heparin (HEP, represented by *diamonds*), chondroitin sulfate A (CSA, represented by *rectangles*), and chondroitin sulfate C (CSC, represented by *triangles*) were analyzed. **b** Various molecular weights of DS (DS500, represented by *diamonds*; DS20, represented by *rectangles*; DS10, represented by *triangles*; and DS5, represented by *asterisks*) were analyzed

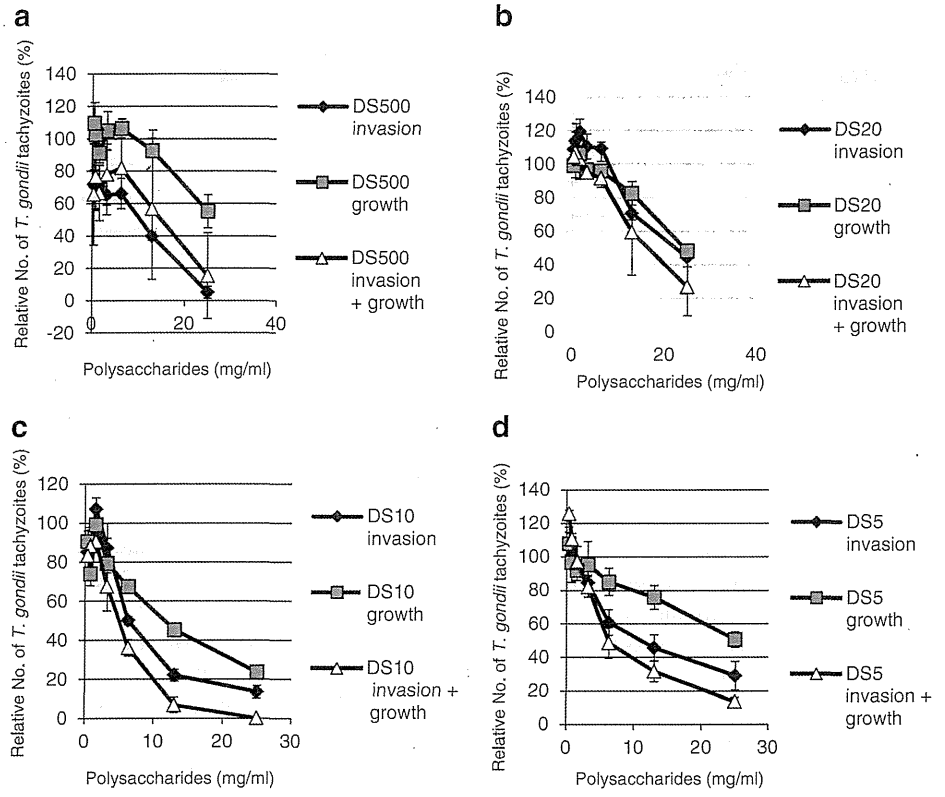

Fig. 3 Invasion and/or growth inhibition analysis by using the β-galactosidase assay. Purified *T. gondii* tachyzoites were incubated with host cells for 30 min in the assay medium containing increasing concentrations of DS samples (invasion, shown as *diamonds*), extensively washed with PBS, and then incubated with normal assay medium at 37 °C for up to 24 h. For the growth inhibition analysis, tachyzoites were incubated with host cells for 30 min in the assay medium that lacked DS samples, extensively washed with PBS, and then incubated with the assay medium containing an increasing concentration of DS samples (growth, shown as rectangles) in a 96-well plate. *Triangles* show samples incubated with the DS additives at both the invasion and growth stages. After the 24-h incubation, the 96-well plate was washed with PBS, and *T. gondii* growth was detected by using a β-galactosidase activity. In this study, various molecular weights of DS samples (**a** DS500, **b** DS20, **c** DS10, **d** DS5) were added at the invasion and/or growth stage

results (Fig. 3a–d). Although DS500 effectively inhibited invasion, its effect on growth appeared to be weak (Fig. 3a). By contrast, the low molecular weight DSs effectively inhibited both invasion and growth by endodyogeny (Fig. 3b). DS10 was the most effective inhibitor of *T. gondii* (Figs. 1b and 3a, c), because it appears to both disrupt invasion and decelerate parasite growth inside the host cells. These results led us to use this low molecular weight DS for the animal experiments described below.

We also checked the possibility that the polysaccharides used in this study are directly inhibiting β-galactosidase activity (Fig. 4a, b). These results showed that polysaccharides used in this study have no inhibiting effect on β-galactosidase activity.

Assessment of the infection inhibition effects of DS10 in vivo by using quantitative PCR

To confirm the effect of DS in vivo, we performed experiments in mice. The general scheme of these animal experiments is shown in Fig. 5. Briefly, 1.0×10^3 *T. gondii* tachyzoites were inoculated intraperitoneally and 2.5 mg of DS10 was administrated simultaneously to the mice. Three days after infection, the mice were euthanized and tissues were collected for parasite quantification. *T. gondii* tachyzoites in the lungs and liver of the control group mice (injected with PBS instead of DS10) were detected, as shown in Table 1. On the other hand, no *T. gondii* tachyzoites were detected in the lungs and liver of the DS10-injected mice (Table 1), suggesting that DS10 inhibits the infection of *T. gondii* tachyzoites in vivo. These animal experiments also showed that simultaneous intraperitoneal injection of DS10 and *T. gondii* tachyzoites inhibits *T. gondii* infection.

Discussion

In this study, we analyzed the effects of various sulfated polysaccharides on the invasion and growth (endodyogeny in host cells) of *T. gondii* tachyzoites. GAGs, such as heparin, may function as receptors for *T. gondii* infection, and in experimental systems, they may competitively inhibit the

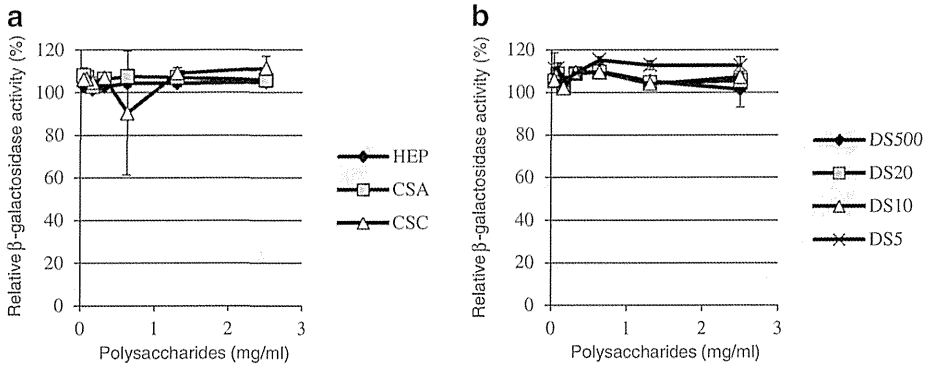

Fig. 4 Validation of the influence of various polysaccharides for β-galactosidase activity. Aliquots of freshly prepared *T. gondii* 2F lysate were mixed with lysis buffer containing increasing concentrations of various polysaccharides, and β-galactosidase activity was detected by colorimetric reaction. **a** Heparin (HEP, represented by *diamonds*), chondroitin sulfate A (CSA, represented by *rectangles*), and chondroitin sulfate C (CSC, represented by *triangles*). **b** DS500 (represented by *diamonds*), DS20 (represented by *rectangles*), DS10 (represented by *triangles*), and DS5 (represented by *asterisks*)

interaction between the *T. gondii* tachyzoites and the host cell surface when administered at high concentrations over a short time period. In this study, the GAGs we analyzed (heparin, CSA, and CSC) had an inhibitory effect on infection, but the efficiency of inhibition was less than 50 % in the 24-h incubation study. In contrast, the various DS molecules used in this study showed more than 50 % inhibition of *T. gondii* invasion and growth. The effects of these DS samples were significant under the 24-h incubation, suggesting that the interactions of DS molecules with *T. gondii* tachyzoites may be stronger than those of GAGs. Thus, DS may be a more effective antagonist than GAG. Moreover, these DS molecules also effectively inhibited the invasion of *T. gondii* tachyzoites in a short-term incubation study (i.e., after a 30-min infection, uninfected parasites were washed out, see Fig. 3a–d).

The results of this study also showed that these DS molecules, particularly the low molecular weight DSs, may act not only on the initial host–parasite interaction (from attachment to invasion) but also on parasite growth inside the host cells (endodyogeny). The mechanistic basis for the inhibitory effect of low molecular weight DSs on the growth of *T. gondii* in host cells is unclear, but two different mechanisms are possible which are as follows: (1) low molecular weight DS may be incorporated into the host cell and interact directly with host cell components and/or the *T. gondii* tachyzoite itself, or (2) DS molecules may have an indirect effect on *T. gondii* tachyzoites from the outside of the host cell via an as yet unidentified pathway through the host cell surface. A previous study reported that it is difficult for high molecular weight DS to cross membranes (Kitajima et al. 1999), and given our finding that the effect of DS500 on *T. gondii* endodyogeny was weak, we believe that these data suggest that the mechanism may be more probable. Further studies are needed to elucidate the precise mechanism of action of DS inhibition of *T. gondii* infection and growth.

We initially postulated that DS500 would show the most potent effect among the DSs tested. However, DS10 turned

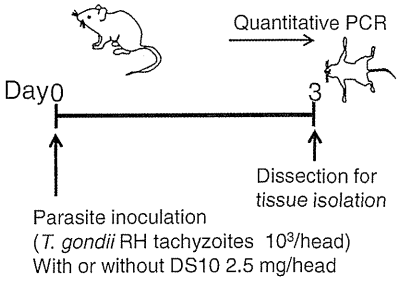

Fig. 5 Infection and growth inhibition analysis in vivo. Schematic summary of the animal experiments performed in this study

Table 1 Detection of parasites by using quantitative PCR

Sample name	Organ	*T. gondii*/g	SD
	Lung		
PBS[a]-1		8,428.781	594.5722
PBS[a]-2		2,574	226.4541
PBS[a]-3		4,951.389	839.915
DS10[b]-1		ND	
DS10[b]-2		ND	
DS10[b]-3		ND	
	Liver		
PBS[a]-1		159,649.1	57,322.14
PBS[a]-2		82,744.11	21,667.22
PBS[a]-3		46,557.33	17,643.48
DS10[b]-1		ND	
DS10[b]-2		ND	
DS10[b]-3		ND	

ND not detected

[a] PBS-: control mice, which were not administrated with additive agents

[b] DS10-: mice administrated with DS10 via intraperitoneal injection and simultaneously inoculated with *T. gondii*